X-ray Absorption Spectroscopy of the Zinc Site in tRNA-Guanine Transglycosylase from *Escherichia coli*†

George A. Garcia,*,‡ David L. Tierney,§ Shaorong Chong,‡,|| Kimber Clark,§ and James E. Penner-Hahn*,§

Interdepartmental Program in Medicinal Chemistry, College of Pharmacy, and Department of Chemistry, University of Michigan, Ann Arbor, Michigan 48109-1065

Received October 6, 1995; Revised Manuscript Received December 15, 1995⊗

ABSTRACT: A key step in the post-transcriptional modification of tRNA with queuine in *Escherichia coli* is the exchange of the queuine precursor, $preQ_1$ into tRNA. This reaction is catalyzed by tRNA-guanine transglycosylase (TGT). We have previously shown that the *E. coli* TGT is a zinc metalloprotein [Chong *et al.* (1995) *Biochemistry 34*, 3694−3701]. Site-directed mutagenesis studies indicated that cysteines 302, 304, 307 and histidine 317 constitute the four ligands to the zinc. The involvement of histidine 317 is somewhat confounded by the presence of histidine 316. We have examined the zinc site in TGT (wt) and TGT (H317C) by X-ray absorption spectroscopy. The TGT (wt) data are most consistent with a tetracoordinate zinc with one nitrogen and three sulfur ligands. Interestingly, the data for TGT (H317C) are also consistent with a tetracoordinate zinc with one nitrogen and three sulfur ligands. The outer shell imidazole scattering for TGT (H317C) appears to be somewhat more ordered than that for TGT (wt), consistent with our previous suggestion that the wild-type enyzme may exist in two conformations the predominant one involving histidine 317 liganding to the zinc and the minor conformer involving histidine 316 liganding to the zinc. The minor conformer, with histidine 316 coordinating the zinc, appears to have an overall conformation that is subtly different from that of the wild-type enzyme. While TGT (H317C) has kinetic parameters very similar to the wild-type, it does not form the homotrimer quaternary structure of the wild-type. TGT (H317A) has previously [Chong *et al.* (1995) *Biochemistry 34*, 3694−3701] been found to contain a significant amount of zinc, but is essentially inactive. This suggests that careful analysis of EXAFS data can reveal subtle conformational changes in metal binding sites that are not observed in more common probes of protein conformation such as CD spectroscopy.

Excepting iron, zinc is perhaps the most abundant metal ion found in proteins. The phenomenon of zinc as both a catalytic and a structural component in enzymes and as a structural component in nucleic acid-binding proteins has been the subject of recent reviews (Berg, 1990; Vallee & Auld, 1990). The zinc-finger motif was first discovered in transcription factors, proteins that bind to specific DNA sequences (Klug & Rhodes, 1987). These motifs usually contain two cysteine and two histidine residues that ligand to the zinc ion in a tetrahedral fashion. More recently four cysteine and three cysteine/one histidine type zinc-finger motifs have been found in proteins that bind to RNA (Miller & Schimmel, 1992). The exact role of the zinc-finger motifs in RNA-binding proteins is still unclear.

A key step in the post-transcriptional modification of tRNA with queuine in *Escherichia coli* is the exchange of the queuine precursor, $preQ_1$ into tRNA, replacing the genetically encoded guanosine-34 in the anticodon (Kersten & Kersten, 1990). This reaction is catalyzed by tRNA-guanine transglycosylase (TGT,[1] E.C. 2.4.2.29) (Okada & Nishimura, 1979, Singhal, 1983). In *E. coli*, TGT catalyzes the incorporation of the queuine precursor $preQ_1$ [7-(aminomethyl)-7-deazaguanine] into tRNA. This precursor is further elaborated to queuine by two subsequent enzymic reactions (Slany & Kersten, 1994). Many of the aspects of tRNA recognition by the *E. coli* TGT have been elucidated (Curnow & Garcia, 1994, 1995; Curnow *et al.*, 1993; Mueller & Slany, 1995; Nakanishi *et al.*, 1994). Recent studies on a series of synthetic 7-deazaguanines have revealed that the *E. coli* TGT tolerates a wide diversity of substituents (isosteric, or nearly so, to the aminomethyl group of $preQ_1$) at the 7-position (Hoops *et al.*, 1995a). These studies have led to the design and characterization of a mechanism-based inhibitor of the TGT reaction (Hoops *et al.*, 1995b).

We have previously reported that TGT from *E. coli* is a zinc metalloprotein (Chong *et al.*, 1995). While the exact role of the zinc domain in TGT is not known, biochemical characterization of site-directed mutants and sequence homology between the *E. coli* TGT and the TGT from *Zymomonas mobilis* (Reuter & Ficner, 1995) indicated that cysteines 302, 304, 307 and histidine 317 constitute the four ligands to the zinc atom (Chong *et al.*, 1995). However,

†This work was supported in part by NIH Grants GM45968 (G.A.G.) and GM38047 (J.E.P.H.) and a training grant-fellowship (K.C.). SSRL is operated by the Department of Energy, Office of Basic Energy Sciences, Division of Chemical Sciences, with additional support from the NIH, Biomedical Resource Technology Program, Division of Research Resources and the Department of Energy, Office of Health and Environmental Research.

‡ Medicinal Chemistry.

§ Department of Chemistry.

|| Present address: New England Biolabs, 32 Tozer Rd., Beverly, MA 01915-5599.

⊗ Abstract published in *Advance ACS Abstracts,* February 15, 1996.

[1] Abbreviations: TGT, tRNA-guanine transglycosylase; DTT, dithiothreitol; HEPES, hydroxyethylpiperazineethylsulfonate; TCA, trichloroacetic acid; ICP-AES, inductively coupled plasma atomic emission spectrometry; XAS, X-ray absorption spectrometry; EXAFS, extended X-ray absorption fine structure.

0006-2960/96/0435-3133$12.00/0

the evidence for the involvement of histidine 317 is less clear than for the other three ligands. One mutant, TGT (H317A), while lacking activity, still binds a significant amount of zinc (ca. 50% that of the wild-type).

In order to further investigate the structure of the zinc binding site in TGT, we have undertaken an X-ray absorption study of the TGT-bound zinc. Additional mutants were made, and EXAFS data were collected for one of those mutants. The EXAFS data indicate that the TGT-bound zinc has one nitrogen and three sulfur ligands, consistent with the previous conclusions (Chong *et al.*, 1995). Interestingly, when the natural histidine ligand (H317) is changed to cysteine, the enzyme appears to choose the adjacent histidine (H316) as the fourth ligand. This suggests that ligand substitution in TGT is not a simple process, consistent with the results recently reported for the zinc site in a "designed" protein (Klemba & Regan, 1995).

MATERIALS AND METHODS

Buffers, DTT, and $MgCl_2$ were purchased from Sigma. [8-^{14}C]Guanine was from Moravek Biochemicals. Homogeneous TGT was prepared from an overexpressing clone as described previously (Chong & Garcia, 1994b; Garcia *et al.*, 1993). Full-length $tRNA^{Tyr}$ (ECY2) was prepared via *in vitro* transcription as described previously (Curnow *et al.*, 1993). Oligonucleotides were synthesized at the University of Michigan Biomedical Resources Core Facility.

Preparation of TGT Mutants. The TGT mutants H316A, H317A, and the H316/317A double mutant were from Chong *et al.* (1995). TGT (H317C) and the double-mutant TGT (H316A/H317C) were prepared via a preferential PCR method (Chong & Garcia, 1994a) using mutagenic oligonucleotides GCA ACG GTC AAG ACA ATG CAA GTA AGC and GTT GCA ACG GTC AAG GCA TGC CAA GTA AGC (mutant codons underlined), respectively. Purifications of the mutant proteins were carried out as previously described (Chong *et al.*, 1995).

Physical Characterization of the Protein. The physical characterization of the protein was carried out as previously described (Chong *et al.*, 1995). The protein concentrations were determined by measuring the absorption at 280 nm and using a corrected absorption coefficient for TGT. Protein concentrations were also determined using the Bradford assay (Bio-Rad) with bovine serum albumin (BSA) as the standard protein. Total amino acid analysis was performed by the University of Michigan Biomedical Resources Core Facility. Duplicate determinations at two different TGT concentrations were used to determine correction factors for the UV and Bradford assays. The corrected absorption coefficient at 280 nm for TGT is 1.14 mg/OD. The correction factor for the Bradford assay is 0.79. The zinc concentrations were determined by inductively coupled plasma atomic emission spectrometry (ICP-AES). The circular dichroism (CD) spectra were measured on 0.1 mg/mL solutions of protein in 2 mM phosphate buffer (pH 7.5) in a Jasco J-710 spectropolarimeter. The native PAGE was performed following the vendor's protocols (Pharmacia Phast System) for 8%−25% gradient gels (Coumassie Blue staining) with the exception that the temperature was maintained at 5 °C.

Enzyme Assays. An aliquot of the enzyme preparation was added to a reaction mixture (400 μL total volume) containing 100 mM HEPES (pH 7.5), 20 mM $MgCl_2$, various concentrations of both [8-^{14}C]guanine (specific activity: 56 mCi/mmol) and $tRNA^{Tyr}$. The reaction mixtures were incubated at 37 °C, and aliquots (75 μL) were taken at various time points. Upon removal from the reaction mixture the tRNA was precipitated by adding 2 mL of a 5% trichloroacetic acid (TCA) solution. The precipitates were then collected on glass fiber filters (Whatman GF/C). The filters were then rinsed, dried, and quantitated via liquid scintillation counting. Initial velocities were determined by linear regression of DPM versus time plots and were replotted versus substrate concentration to obtain the kinetic parameters. Specific activities were determined by replicate assays (as above) in the presence of 10 μM [8-^{14}C]guanine and 10 μM $tRNA^{Tyr}$.

XAS Measurements. Approximately 40 mg of TGT (wt) was precipitated by addition of ammonnium sulfate to 75% saturation. The pellet was rinsed with buffer, and ca. 1/2 of the pellet was loaded into a lucite cuvette (ca. 40 μL volume) with 40 μm Kapton windows. After XAS measurements, approximately equal amounts of pellet slurry from the EXAFS sample and from the unused portion were individually resuspended in 1 mL of 10 mM HEPES buffer (pH 7.5). These were then analyzed for enzyme activity, zinc content, and protein concentration as described above. The TGT (H317C) mutant was prepared for XAS measurements in an identical fashion; however, it was not characterized after XAS.

X-ray absorption data were measured at the Stanford Synchrotron Radiation Laboratory (SSRL), using a wiggler beam line (VII-3) equipped with an Si(220) double-crystal monochromator. Harmonic rejection was accomplished by detuning the monochromator to 50% maximum intensity. All protein data were measured as fluorescence excitation spectra with a 13-element solid state Ge detector array run at a total incident count rate of <40 kHz per channel. The windowed count rates (Zn Kα fluorescence) were ca. 1 kHz per channel. Samples were held at 10 K in an Oxford liquid helium cryostat during XAS measurements.

EXAFS spectra were measured with 10 eV steps below the edge (9300−9630 eV), ∼0.5 eV steps in the edge region (ca. 9630−9700 eV), and 0.05 Å^{-1} steps in the k range 2−13 Å^{-1}. Integration times varied from 1 s in the pre-edge region to 20 s at k = 13 Å^{-1} for a total integration time of approximately 45 min per scan. Total exposure time was typically 6 h for protein samples.

Individual scans from each detector channel were examined to confirm the absence of artifacts and averaged to give the final spectra. The EXAFS spectra represent the average of eight scans for TGT (wt) and seven scans for TGT (H317C), each scan being the average of 8−10 channels. For each sample, the total Zn Kα fluorescence counts were approximately 2×10^6 at $k = 13$ Å^{-1}. X-ray energies were calibrated by simultaneous measurement of the absorption spectrum of a zinc foil. The first inflection point of the Zn foil was assigned as 9659 eV.

EXAFS background subtraction was accomplished by fitting a first-order polynomial to the pre-edge region and a two-region cubic spline above the edge. Data were converted from energy to k space using

$$k = \sqrt{2m_e(E - E_o)/\hbar^2}$$

with E_0 set at 9675 eV. The resultant EXAFS data were Fourier transformed over the region k = 2.0−12.0 Å^{-1}. The

first shell was back-transformed ($R = 0.7-3.0$ Å for both) over the same k range. The resulting EXAFS data (ca. 15 degrees of freedom) were fitted to eq 1 using a nonlinear least-squares algorithm.

$$\chi(k) = \sum \frac{N_s A_s(k) \mathrm{Sc}}{kR_{as}^2} \exp(-2k^2\sigma_{as}^2) \exp(-2R_{as}/\lambda) \sin[2kR_{as} + \phi_{as}(k)] \quad (1)$$

In eq 1, N_s is the number of scattering atoms within a shell, $A_s(k)$ is the back-scattering amplitude of the absorber−scatterer pair, σ^2 is the mean square deviation of the absorber−scatterer bond length R_{as}, $\phi_{as}(k)$ is the phase shift, λ is the photoelectron mean free-path, and the sum is taken over all shells contributing to the EXAFS. The parameter Sc is the scale factor, which is, in principle, specific to the absorber−scatterer pair. The program FEFF v. 6.01 (Rehr *et al.*, 1991, 1992) was used to calculate *ab initio* amplitude and phase functions, $A_s(k) \exp(-2R_{as}/\lambda)$ and $\phi_{as}(k)$. Calculations were done for a single zinc−nitrogen interaction at 2.05 Å and a single zinc−sulfur interaction at 2.35 Å. The scale factor, Sc, and the shift in E_0 relative to 9675 eV were calibrated by fitting compounds of known structure[2] (Clark, 1993) and held fixed at their optimum values (Sc = 0.85 and $E_0 = 9$ for zinc−nitrogen, and Sc = 1.02 and $E_0 = 9$ for zinc−sulfur) during fits to protein data. For each sample, a series of fits were carried out holding the total zinc coordination number fixed at 4, while varying the number of nitrogens in steps of 0.25.

For each individual fit, R and σ were varied for both shells while all other parameters were held fixed. Data were analyzed by the method of Clark *et al.* [2] [see also Clark, (1993)] in order to test the effect of mutating histidine 317 to cysteine on the zinc environment. The percent improvement in the mean-square deviation between the data and the fit (% I) as a function of the percentage of sulfur contribution was calculated according to eq 2.

$$\% \mathrm{I} = \left(\frac{F_{4S} - F_i}{F_{4S}}\right) \times 100 \quad (2)$$

In eq 2, F_{4S} represents the mean-square deviation for a fit of one shell of four sulfurs (two variable parameters) and F_i represents the deviation for a two-shell fit including nitrogen contributions (four variables). These results were compared to a fit with two shells of two sulfurs each, which represents the improvement expected for simply doubling the number of variable parameters.

EXAFS data for TGT (wt) were measured on two separate samples. The EXAFS data for TGT (H317C) were measured on a single preparation of the protein. Therefore, to ensure the lack of artifacts, the first half and the second half of the scans for TGT (H317C) were averaged and fitted in the same manner as the overall average. Each half of the data gave results indistinguishable from the overall average.

RESULTS

Physical Characterization of Wild-Type and Mutant TGTs. Each of the mutant TGTs were overexpressed, purified, and characterized. The circular dichroism (CD) spectra of TGT (wt) and TGT mutants are shown in Figure 1. The spectra for TGT (wt), H316A, H317A, and H316/317A were from Chong *et al.* (1995). The spectra of TGT (H316A) and TGT (H317C) are very similar to the wild-type, while the spectra for TGT (H317A) and TGT (H316/317A) are significantly different. The CD spectrum for TGT (H316A/H317C) was not determined.

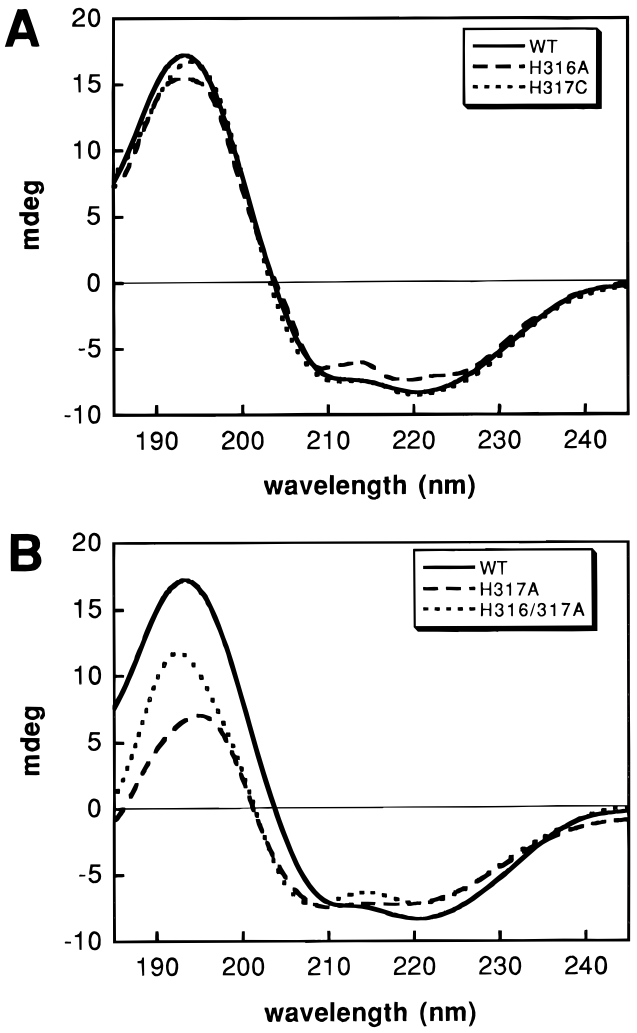

FIGURE 1: CD-spectra of TGT (wt) and mutants. Spectra were recorded as previously described (Chong *et al.*, 1995). The spectra for TGT (wt), H316A, H317A, and H316/317A were from Chong *et al.* (1995).

Native PAGE of TGT (wt), TGT (H317C), and TGT (H316/317A) in the absence and presence of tRNA is shown in Figure 2. TGT (wt) shows the characteristic band shift (Curnow & Garcia, 1994) from a homotrimer to a monomer·tRNA complex (lanes 2 and 3). TGT (H317C) alone migrates to an apparent monomer M_r; however, in the presence of tRNA, TGT (H317C) migrates to a position identical to that of the TGT (wt) monomer·tRNA complex. TGT (H316/317A) does not form the homotrimer nor does it appear to form any complex with tRNA. TGT (H316A/H317C) behaves identically to TGT (H316/317A) on native PAGE, indicating that it also does not form the homotrimer nor the complex with tRNA (data not shown).

The zinc content for TGT (H317C) was found to be 0.49 and for TGT (H316A/H317C) to be 0.01 zinc/TGT monomer. The zinc contents for TGT (wt), H316A, H317A, and

[2] K. Clark, D. L. Tierney, K. Govindaswamy, E. Gruff, C. Kim, J. Berg, S. Koch, and J. E. Penner-Hahn, unpublished.

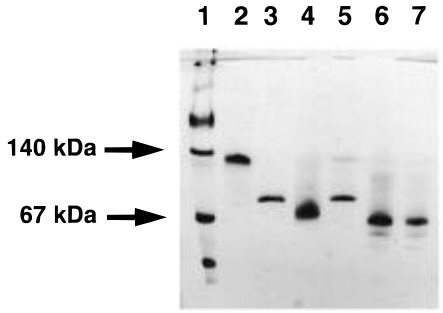

FIGURE 2: Native PAGE analysis of quaternary structure and tRNA binding by TGT (wt) and mutants. Native PAGE was run on a Phastsystem (Pharmacia) as previously described (Chong *et al.*, 1995). Lane 1, MW standards; lane 2, TGT (wt); lane 3, TGT (wt) + tRNA; lane 4, TGT (H317C); lane 5, TGT (H317C) + tRNA; lane 6, TGT (H316/317A); and lane 7, TGT (H316/317A) + tRNA.

Table 1: Kinetic Parameters and Zinc Contents for TGT (wt) and TGT (H317C)[a]

	K_M (μM)	V_{max} (10^{-6} M s^{-1} mg^{-1})	V_{max}/K_M (s^{-1} mg^{-1})	V_{max}/K_M ratio	zinc content
TGT (wt)					0.75
$tRNA^{Tyr}$	2.0 (0.12)	11.0 (0.2)	5.5 (0.5)	1	
guanine	1.2 (0.13)	10.1 (0.3)	8.4 (1.3)	1	
TGT (H317C)					0.49
$tRNA^{Tyr}$	6.5 (0.5)	7.4 (0.2)	1.1 (0.2)	0.2	
guanine	1.6 (0.3)	7.2 (0.3)	4.5 (1.3)	0.5	

[a] The kinetic parameters were determined using the guanine exchange assay as described in Materials and Methods and previously (Chong *et al.*, 1995). The zinc contents were calculated using zinc concentrations measured by ICP-AES analysis and protein concentrations determined using a UV absorption coefficient corrected by total amino acid analysis as previously described (Chong *et al.*, 1995). The numbers in parentheses are standard errors.

Table 2: TGT Activity, Zinc Content, and Protein Concentration before and after XAS[a]

TGT	relative activity[b]	[Zn] (μM)	[protein] (μM) UV	Bradford	total AA
before XAS	100	9.4 (± 0.3)	10.1	12.9	10.3
after XAS	78	8.0 (± 0.2)	28.2	4.46	4.70

[a] Approximately equal amounts of the ammonium sulfate slurrys were resuspended in 1 mL of HEPES buffer (pH 7.5). [b] Equal aliquots (15 μL) of resuspended samples were assayed for TGT activity as described in Materials and Methods. Values reported are relative activities per aliquot. Zinc content and protein concentrations were performed as described in Materials and Methods. The UV and Bradford protein concentrations are uncorrected.

H316/317A were previously determined to be ca. 0.75, 0.76, 0.35, and 0.02 zinc/TGT monomer, respectively (Chong *et al.*, 1995). It was previously shown that TGT (H317A) and TGT (H316/317A) are inactive and that TGT (H316A) has essentially wild-type activity (Chong *et al.*, 1995). While TGT (H316A/H317C) was found to be inactive (data not shown), TGT (H317C) is active. The kinetic parameters for TGT (H317C) were determined and are compared to those for TGT (wt) in Table 1.

EXAFS of TGT-Bound Zinc. The enzyme activity and zinc concentration of the TGT (wt) sample used in the EXAFS measurements were slightly reduced after XAS (Table 2). This apparent reduction is almost certainly due to the fact that only approximately equal amounts of the ammonium sulfate pellets were resuspended. Protein concentrations were

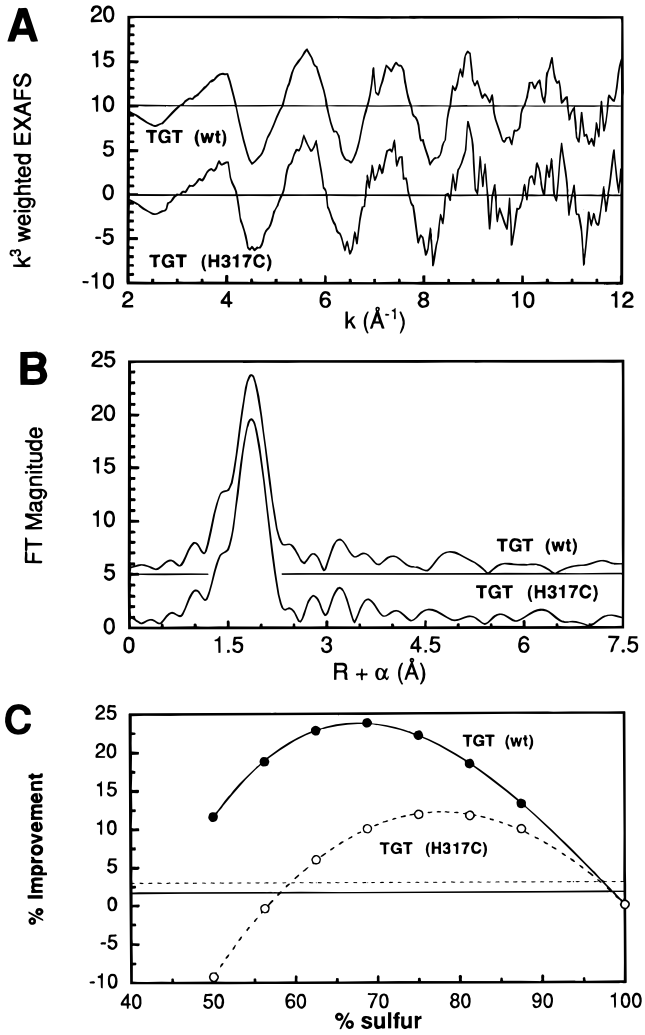

FIGURE 3: EXAFS analysis of TGT (wt) and TGT (H317C). Panel A: EXAFS spectra of TGT (wt), top, and TGT (H317C), bottom. Panel B: Fourier transform of EXAFS spectra of TGT (wt), top, and TGT (H317C), bottom. Panel C: Percent improvement of fit of the two-shell, sulfur−nitrogen model (denoted as percent sulfur) to the EXAFS spectra for TGT (wt), top, and TGT (H317C), bottom. The horizontal lines represent the % I for the 2S + 2S threshhold fits with the same line types as the data.

going to be used to determine specific activites and zinc contents before and after XAS. However, the UV method gave an apparent three-fold increase in protein concentration for the XAS sample. The Bradford assay (Bio-Rad) and total amino acid analysis (Table 2) were also used to determine protein concentrations.

The background-subtracted EXAFS data for TGT (wt) and the H317C mutant are shown in Figure 3A. From the figure it is clear that the EXAFS amplitude and frequency are similar. The corresponding Fourier transforms (FTs) are shown in Figure 3B. The FTs show a single well-resolved peak at $R + \alpha \approx 1.9$ Å. The magnitude of the main peak is indicative of high-Z scatterers (*i.e.*, sulfur). Comparison of the EXAFS and the FTs with model data (not shown) suggests that the coordination sphere of the zinc in both samples is consistent with primarily sulfur ligands. However, from the appearance of the data, it is not clear whether the average zinc environment is all sulfur or a mixture of sulfur and nitrogen. The large EXAFS amplitude associated with sulfur ligands makes quantitation of low-Z scatterers difficult (Clark, 1993; Tsang *et al.*, 1989).

Table 3: Curve Fitting Results for TGT[a]

sample[b]	R_S (Å)	$\sigma_s^2 \times 10^3$ (Å^2)	R_N (Å)	$\sigma_N^2 \times 10^3$ (Å^2)	S_{max} (%)
TGT (wt)					
set 1	2.28	4.0	2.08	7.7	76
set 2	2.28	3.7	2.04	5.8	72
TGT (H317C)					
set 1	2.29	4.1	2.08	4.4	74
set 2	2.28	4.0	2.10	9.1	71
average	2.28	4.1	2.09	6.6	73

[a] Best fits to Fourier-filtered EXAFS data for a ZnS_3N model. Fits to unfiltered data gave similar results. R and σ^2 are the average bond length and the Debye−Waller factor, respectively, for each shell. S_{max} is the % S giving the best fit (see text). [b] For TGT (wt), two independent data sets were measured, with data set 1 having significantly better signal/noise ratio. For TGT (H317C), the single data set was divided into two parts for analysis purposes, to test the effect of random noise on the results.

The EXAFS spectra of metal ions that are ligated to histidine imidazoles are characterized by long distance ($R + \alpha > 3$ Å) scattering from the outer atoms of the imidazole ring (Strange *et al.*, 1987). The FT for TGT (H317C) shows three outer peaks, at $R + \alpha \approx 2.8$, 3.2, and 3.6 Å, that are clearly above the noise level. These are very similar to the peaks seen for authentic $Zn(Cys)_3His$ peptide (Clark, 1993) and for zinc (*N*-methylimidazole)$_4^{2+}$ and have an amplitude consistent with approximately one imidazole per Zn. There are also outer shell peaks in the TGT (wt) FT; however, these differ slightly in both position and relative amplitude from the typical imidazole scattering.

Quantitative curve fitting results for filtered first shell data are given in Table 3, and the percent improvement (% I) as a function of percent sulfur (% S) is shown graphically in Figure 3C. The horizontal lines in Figure 3C correspond to the % I that is observed for a two-shell fit using sulfurs only (2S + 2S). This represents the % I to be expected simply by doubling the number of variable parameters. Both TGT (wt) and TGT (H317C) display maxima at ca. 75% sulfur that are significantly above the 2S + 2S threshhold. This is typical of % I plots that are found for $Zn(Cys)_3His$ proteins and models (Clark, 1993; Landro *et al.*, 1994) and is distinct from the behavior for $Zn(Cys)_4$ data, where the % I is greatest for the 2S + 2S fit. While S_{max} (the % S giving the highest % I) for TGT (H317C) is shifted to slightly higher % S compared to TGT (wt), both are consistent with a $(Cys)_3His$ environment. The refinements of σ_N and σ_S, in the fits that include nitrogen and σ_S for the 2S + 2S fit, are also consistent with this ligation.

DISCUSSION

Previously, we have used site-directed mutagenesis and physical characterization of the resulting mutant proteins to determine that the tRNA-guanine transglycosylase (TGT) from *E. coli* contains one tightly bound zinc atom per TGT monomer and to identify the enzymic ligands to the zinc as cysteines 302, 304, 307 and histidine 317 (Chong *et al.*, 1995). The zinc site in TGT appears to be filling a solely structural role. While the evidence for the involvement of the cysteines was unambiguous, that for the involvement of histidine 317 was less so. The results with the TGT (H316A), TGT (H317A), and TGT (H316/317A) mutants have strongly suggested that histidine 317 is the fourth ligand to the zinc. While the H317A mutant was essentially inactive, it did contain a significant amount of zinc (ca. 0.35 Zn/monomer). This suggested that the histidine in position 316 was serving as the fourth ligand to the TGT-bound zinc when H317 was removed, but that this interaction gave a significantly altered conformation that did not yield an active enzyme. To further study the zinc binding site in TGT, we have constructed two additional mutants, TGT (H317C) and TGT (H316A/H317C), and subjected them to the same physical and kinetic characterization.

The circular dichroism spectum of TGT (H317C) is essentially identical to that of the wild-type and TGT (H316A), indicating that there has been no gross change in the secondary structural elements of the enzyme (Figure 1A). This is in contrast to the change in CD spectra for the TGT (H317A) and TGT (H316/317A) mutants relative to the wild-type (Figure 1B). ICP-AES analysis indicates that TGT (H317C) contains a slightly lower content of zinc than the wild-type, which is also consistent with the lack of gross changes in enzyme tertiary structure. However, native PAGE reveals that TGT (H317C) does not exist in the homotrimeric (of 42.5 kDa subunits) quaternary state that we have observed for the wild-type; rather, it appears to exist as a monomer. This monomeric TGT (H317C) does exhibit a band shift on native PAGE to a monomer·tRNA complex identical to that for the wild-type TGT (Figure 2). Recent gel-filtration chromatography experiments on the *E. coli* TGT (wt) indicate that the size of the enzyme (as judged by retention volume) is dependent upon the enzyme concentration at concentrations less than 1 mg/mL (Reuter & Ficner, 1995). Although the concentration at which the monomer species predominates was not determined, the results suggest that the trimerization that we have observed to be specific and reversible *in vitro* may not be physiologically relevant. The present results with TGT (H317C) are consistent with the dispensibility of homotrimer formation for TGT activity.

The kinetic parameters for TGT (H317C) were determined for both tRNA and guanine substrates (Table 1). The V_{max} for TGT (H317C) is reduced (ca. 70%) compared to the V_{max} for the wild-type. However, this reduction in V_{max} closely parallels the reduction in zinc content (ca. 65%) and therefore is most likely due to a reduction in the amount of active, zinc-containing enzyme and not to a true change in k_{cat}. The K_m for guanine is, within experimental error, unchanged from that of the wild-type. The K_m for tRNA is ca. 3-fold higher than the wild-type. This change in K_m for tRNA may reflect a subtle change in protein conformation that is not observed in the CD spectra. Presumably, it is this change in conformation that is also responsible for the lack of trimerization of the TGT (H317C) mutant.

The present results with TGT (H317C) raise the following question: Has the nature of the fourth ligand to the zinc changed from histidine to cysteine 317 or is histidine 316 serving as the fourth ligand in a conformation different from TGT (H317A) that allows for enzyme activity essentially identical to that of the wild-type? In order to answer that question and to provide further evidence for the C_3H ligand structure for the wild-type TGT we have performed extended X-ray absorption fine structure (EXAFS) analyses on TGT (wt) and TGT (H317C).

The enzyme activity and zinc concentration of the TGT (wt) sample used for the EXAFS were only slightly reduced after XAS (Table 2). The apparent changes in protein

concentration are mutually inconsistent and are inconsistent with the lack of change in either enzyme activity or zinc concentration. It is unclear why the protein assays of the XAS sample do not correspond to the enzyme activities and zinc concentrations. It may be that free radicals formed upon exposure of the sample to the X-ray beam have recombined to generate a small fraction of highly absorbing species. The UV spectrum (data not shown) of the XAS sample does show that the 280 nm absorbance peak is larger and slightly shifted to higher wavelength than that of the unused sample. The chromatogram for the total amino acid analysis of the XAS sample shows a large peak at 11.18 min that is not found in the unused sample chromatogram, possibly due to a modified amino acid (data not shown). However, the initial and final EXAFS scans were identical, demonstrating that the Zn site structure was unaffected by any X-ray induced damage.

From Figure 3, it is clear that the zinc coordination sphere contains predominantly sulfur. The fit in Figure 3 and Table 3 assumed a four-coordinate environment. This assumption is confirmed by the finding that the average zinc−sulfur bond length, 2.28 Å, is typical of that seen in four-coordinate Zn complexes and is significantly different than expected for other coordination numbers (Thorp, 1992). The average Zn−S distance in four-coordinate Zn complexes is 2.33 Å. All of the known three-coordinate zinc compounds with sulfur ligands have an average Zn−S bond length ≤2.23 Å, while five- and six-coordinate complexes have Zn−S distances longer than 2.40 Å.

Quantitative analysis of the EXAFS for TGT (wt) is clearly consistent with a $(Cys)_3His$ coordination environment. The S_{max} of ca. 75% sulfur and the maximum % I of ∼20% are in good agreement with results found[2] (Clark, 1993; Landro *et al.*, 1994) for authentic $(Cys)_3His$ zinc peptides. When the EXAFS data for an authentic ZnS_4 site are fitted to a ZnS_3N model, the refined σ_N goes to zero. In no case did σ_N refine to zero in fits to TGT (wt). All of these data give strong support to the conclusion that the zinc site in native TGT is made up of three cysteines and one histidine.

Mutation of histidine 317 to cysteine causes a shift in the percent improvement plot (Figure 3C) to slightly lower % S, with a maximum that is appreciably lower than that for the wild-type. This variation indicates some change in ligation; however, the refined variables (S_{max}, σ_S, and σ_N) remain most consistent with a $(Cys)_3His$ model. The outer shell peaks in the Fourier transform for TGT (H317C) are significantly larger than those in TGT (wt). This indicates a more ordered environment in TGT (H317C) or, alternatively, a more disordered environment in TGT (wt). In the wild-type enzyme, both residues 316 and 317 are histidine and, therefore, are potential ligands to the zinc. The suggestion that both histidines can act as ligands to Zn is supported by the finding that both TGT (H316A) and TGT (H317A) exhibit appreciable (≥0.35 Zn/monomer) Zn binding (Chong *et al.*, 1995). The lower amplitude of the outer shells in the TGT (wt) FT could be reflective of a mixture of species, with an appreciable fraction of the sites utilizing H316 as the fourth zinc ligand and the rest using H317. Minor differences in the Zn−histidine orientation can result in larger changes in the Zn- - -C outer shell distances. In TGT (H317C), only one histidine is present. Thus, the mutant would represent a more homogeneous zinc coordination sphere, and outer shell scattering would appear more ordered.

The EXAFS results suggest that if H317 is not available, then the Zn site undergoes minor changes in geometry (see Figure 3), but retains the overall $(Cys)_3His$ ligation by utilizing H316 as a ligand. An alternate interpretation would be that one of the three other conserved histidines in TGT (60, 77, and 333) serves as the fourth Zn ligand. In this case, the loss of activity in H317A would have to be attributed to conformational changes remote from the Zn site. Mutagenesis will be required to absolutely rule out this possibility (*i.e.*, by mutating each histidine individually to alanine), and such experiments are in progress. However, we consider this possibility remote in view of the fact that replacement of *both* histidine 316 and 317 abolishes Zn binding while replacement of either histidine 316 or 317 alone leaves Zn binding intact. Moreover, it would be difficult to explain how the H317C mutation could affect the Zn site structure (Figure 3C) if this mutation is not at the Zn site.

These results strongly suggest that, when presented with histidine in position 316 and cysteine in position 317, TGT selects the histidine rather than the cysteine to serve as the fourth ligand to the zinc. Consistent with this is our earlier conclusion (Chong *et al.*, 1995) that the histidine at position 316 can serve as the fourth ligand to the zinc when histidine 317 is replaced with alanine. It is unclear why the incorporation of cysteine at position 317 yields an enzyme that is extremely similar to the wild-type in structure and activity whereas alanine in this position results in an inactive enzyme. In an attempt to provide the enyzme with no alternative fourth ligand except a cysteine in position 317, we constructed the TGT (H316A/H317C) double mutant. Unfortunately this mutant does not appear to fold correctly. Although the CD spectrum of this mutant was not determined, native PAGE (not shown) indicates that this mutant does not bind tRNA and activity assays (not shown) indicate that the mutant is inactive. This result is similar to a recent report (Klemba & Regan, 1995) in which mutagenesis experiments were performed to change a histidine ligand to cysteine in a tetrahedrally coordinated zinc site in a designed protein. Klemba and Regan (1995) found that replacement of the histidine with cysteine did not result in the cysteine serving as a ligand to the zinc. The authors concluded that simple amino acid substitution did not place the liganding atom in the correct position to form the tetrahedral coordination sphere around the zinc. It appears likely that a similar ligation change takes place in TGT (H317C).

ACKNOWLEDGMENT

We thank Professor S. Koch (SUNY, Stony Brook) for a gift of some of the Zn model compounds and Dr. T. J. Huston (University of Michigan, Department of Geological Sciences) for the zinc determinations.

SUPPORTING INFORMATION AVAILABLE

Comparison of EXAFS and FTs for best S_3N fits relative to data for TGT (wt) and TGT (H317C) (2 pages). This material is contained in many libraries on microfiche, immediately follows this article in the microfilm version of the journal, can be ordered from the ACS, and can be downloaded from the Internet; see any current masthead page for ordering information and Internet address.

REFERENCES

Berg, J. M. (1990) *J. Biol. Chem. 265*, 6513−5616.

Chong, S., & Garcia, G. A. (1994a) *BioTechniques 17*, 719−725.

Chong, S., & Garcia, G. A. (1994b) *BioTechniques 17*, 686−691.

Chong, S., Curnow, A. W., Huston, T. J., & Garcia, G. A. (1995) *Biochemistry 34*, 3694−3701.

Clark, K. (1993), Ph.D. Thesis, The University of Michigan.

Curnow, A. W., & Garcia, G. A. (1994) *Biochimie 76*, 1183−1191.

Curnow, A. W., & Garcia, G. A. (1995) *J. Biol. Chem. 270*, 17264−17267.

Curnow, A. W., Kung, F. L., Koch, K. A., & Garcia, G. A. (1993) *Biochemistry 32*, 5239−5246.

Garcia, G. A., Koch, K. A., & Chong, S. (1993) *J. Mol. Biol. 231*, 489−497.

Hoops, G. C., Townsend, L. B., & Garcia, G. A. (1995a) *Biochemistry 34*, 15381−15387.

Hoops, G. C., Townsend, L. B., & Garcia, G. A. (1995b) *Biochemistry 34*, 15539−15544.

Kersten, H., & Kersten, W. (1990) in *Chromatography and Modification of Nucleosides, Part B: Biological Roles and Function of Modification* (Gehrke, C., & Kuo, K., Ed.) pp B69-B108, Elsevier, Amsterdam.

Klemba, M., & Regan, L. (1995) *Biochemistry 34*, 10094−10100.

Klug, A., & Rhodes, D. (1987) *Cold Spring Harbor Symp. Quant. Biol. 52*, 473−482.

Landro, J. A., Schmidt, E., Schimmel, P., Tierney, D. L., & Penner-Hahn, J. E. (1994) *Biochemistry 33*, 14213−14220.

Miller, W. T., & Schimmel, P. R. (1992) *Mol. Microbiol. 6*, 1259−1262.

Mueller, S. O., & Slany, R. K. (1995) *FEBS Lett. 361*, 259−264.

Nakanishi, S., Ueda, T., Hori, H., Yamazaki, N., Okada, N., & Watanabe, K. (1994) *J. Biol. Chem. 269*, 32221−32225.

Okada, N., & Nishimura, S. (1979) *J. Biol. Chem. 254*, 3061−3066.

Rehr, J. J., Mustre, d. L. J., Zabinsky, S. I., & Albers, R. C. (1991) *J. Am. Chem. Soc. 113*, 5135−5140.

Rehr, J. J., Albers, R. C., & Zabinsky, S. I. (1992) *Phys. Rev. Lett. 69*, 3397−3400.

Reuter, K., & Ficner, R. (1995) *J. Bacteriol. 177*, 5284−5288.

Singhal, R. P. (1983) *Prog. Nucleic Acids Res. Mol. Biol. 28*, 75−80.

Slany, R. K., & Kersten, H. (1994) *Biochimie 76*, 1178−1182.

Strange, R. W., Blackburn, N. J., Knowles, P. F., & Hasnain, S. S. (1987) *J. Am. Chem. Soc. 109*, 7157−7162.

Thorp, H. H. (1992) *Inorg. Chem. 31*, 1585−1588.

Tsang, H.-T., Batie, C. J., Ballou, D. P., & Penner-Hahn, J. E. (1989) *Biochemistry 28*, 7233−7240.

Vallee, B. L., & Auld, D. S. (1990) *Biochemistry 29*, 5647−5659.

BI952403V